Polymer 118 (2017) 297–304

Contents lists available at ScienceDirect

Polymer

journal homepage: www.elsevier.com/locate/polymer

Pressure dependence of equilibrium melting temperature of poly (lactic acid)

David Rohindra [a, b, *], Keiichi Kuboyama [a], Toshiaki Ougizawa [a]

[a] Department of Materials Science and Engineering, Tokyo Institute of Technology, 2-12-1-S8-33, O-okayama, Meguro-ku, Tokyo 152-8552, Japan
[b] School of Biological and Chemical Sciences, Faculty of Science, Technology and Environment, The University of the South Pacific, Private Mail Bag, Suva, Fiji

ARTICLE INFO

Article history:
Received 1 February 2017
Received in revised form
28 April 2017
Accepted 30 April 2017
Available online 3 May 2017

Keywords:
Poly(lactic acid)
High pressure
Equilibrium melting temperature
Entropy of fusion
Enthalpy of fusion

ABSTRACT

The behavior of the equilibrium melting temperature (T_m^o) of poly(L-lactic acid) with pressure estimated using the Gibbs-Thomson method is presented. Differential scanning calorimetry and a High pressure differential thermal analyzer have been used to determine the melting temperatures of samples isothermally crystallized at atmospheric pressure and at pressures ranging from atmospheric to 300 MPa respectively. Lamellar thickness of the crystals was determined from small angle X-ray scattering. The $\left(\frac{dT_m^o}{dP}\right)_o$ was found to follow the second order polynomial $T_m^o = 206 + 0.309P - 3.86 \times 10^{-4}P^2$. The enthalpy and entropy of fusion of the perfect crystal up to 300 MPa determined through the Clapeyron equation remained more or less similar up to 200 MPa but increased significantly at 300 MPa. The ΔH_f^0 and ΔS^0 at atmospheric pressure were calculated to be 94.5 Jg^{-1} and 0.197 $JK^{-1}g^{-1}$, respectively while the fold surface energy was calculated to be 64×10^{-3} Jm^{-2}.

1. Introduction

Biopolymers are now attracting much attention because they are renewable, and are derived or produced from natural sources and living organisms which create a sustainable industry. These polymers are classed as carbon neutral because the crops from which these biopolymers are derived reabsorb the CO_2 released during their degradation. Biopolymers are mainly polyesters and are finding applications in several areas ranging from packaging to medicine. Among the biopolyesters, poly(lactic acid) (PLA) has been given much attention because it is considered as both biodegradable, adapted for short term packaging application, and biocompatible with living tissues suitable for biomedical applications. PLA synthesis is a multistep process where the monomer lactic acid, largely produced by the fermentation of carbohydrates, is polymerized. There are two main ways to synthesize PLA; one is from the condensation of lactic acid which yields low-molecular weight and the other is from the ring opening polymerization of lactide which yields high molecular weight PLA. PLA biodegrades into harmless natural products through hydrolysis and enzymatic catalysis. Because the raw material is from renewable resources, this polyester is classified as an environmentally friendly material. Mechanically, this polyester is a high strength and high modulus thermoplastic and can be easily processed on standard equipment such as injection, extrusion or blow molding to yield molded parts [1]. PLA has two isomers, the D form, poly(D-lactic acid) (PDLA), and the L form poly(L-lactic acid) (PLLA) and both isomers are crystalline. However, poly(DL-lactic acid) which is the combination of the L and the D form is amorphous. PDLA is expensive compared to PLLA, thus the latter is used for the manufacture of commercial goods. Although PLLA is semicrystalline, the crystallization rate is very slow. This has delayed PLLA's widespread commercial use. Extensive investigations are undertaken to improve the crystallization rate for this polyester [2–6]. Recently, development of stereocomplex of PLLA and PDLA has also progressed with improved properties [7]. Despite the extensive literature available on the crystallization behavior of this polyester, very limited literature [8,9] are available at elevated pressures. Reported works under high pressure on this polyester are through the use of pressurized gas and are mainly on the crystallization and melting behavior [10–12].

According to the European Bioplastics Association [13], only one third of the total lactic acid produced is being used for PLA

* Corresponding author. School of Biological and Chemical Sciences, Faculty of Science, Technology and Environment, The University of the South Pacific, Private Mail Bag, Suva, Fiji.
E-mail address: rohindra_d@usp.ac.fj (D. Rohindra).

http://dx.doi.org/10.1016/j.polymer.2017.04.078
0032-3861/

production annually. This indicates that this polyester has a high potential for development. As the application of this polyester as plastic products increases, it will often be exposed to elevated pressures during processing. Pressure has been shown to affect the crystallization behavior of polymers, therefore, information about crystallization at elevated pressures is important to envisage the processing conditions of this polyester in order to control the physical properties. Of interest, is the behavior of the equilibrium melting temperature (T_m^o) with pressure. The T_m^o is defined as the melting temperature of an infinite stack of extended chain crystals. This entity is one of the most important thermodynamic properties of crystallizable polymers, as it is the reference temperature from which the driving force for crystallization is defined. The lateral growth rate, the fold surface energy and the nucleation rate are all controlled by the degree of supercooling (ΔT) according to the secondary nucleation crystallization growth theory of Lauritzen and Hoffman [14]. ΔT is defined as T_m^o-T_c, where T_c is the crystallization temperature. Due to the difficulty in growing extended chain crystals, T_m^o is normally determined using extrapolative method such as the Hoffman-Weeks (HW) or Gibbs-Thomson plot. The theory related to these methods has been well described in the literature [15–20]. Of these two methods, the Gibbs-Thomson method is considered to give an accurate and reliable estimate of the T_m^o because it is directly derived from thermodynamic arguments with few assumptions used [17–20]. In this method, the polymer is isothermally crystallized at different T_c's and the melting temperatures (T_m's) of the corresponding crystal lamellar thickness (l) are measured. The measured T_m's are plotted against the inverse of (l). The T_m is well known to depend on the crystal form and the lamellar thickness of the crystals. To estimate the accurate value of T_m^o, the T_m should be stable at the corresponding T_c at which it was crystallized, i.e., the crystals should not undergo reorganization, premelting or lamellar thickening during the heating measurement. It has been reported [20] that thin lamellar crystals formed at large supercoolings, when heated at slow heating rates, readily undergo thickening. To overcome this shortcoming, thick lamellar crystals crystallized at small supercoolings should be used and scanned at faster heating rates to determine the T_m. However, the latter condition contributes to thermal lag, which needs to be corrected, and methods for eliminating this is well described in the literature [16,18].

At present, the information on the pressure dependence of the T_m^o of PLLA and the thermodynamic data at high pressures are lacking because of the difficulty in growing extended chain crystals and measuring the T_m of such crystals at elevated pressures directly, except for polyethylene, which can grow extended chain crystals at pressures above 300 MPa [21–26].

In this study, our objective is how best can we determine the T_m^o of PLLA using the Gibbs-Thomson method at elevated pressures and calculate the enthalpy and entropy of fusion at different pressures using the Clapeyron equation. To the best of our knowledge, this is the first experimental approach to measure the pressure dependence of melting temperature and the thermodynamic variables of PLLA using this technique. A lot of attention has been focused on minimizing the effects of lamellar thickening and thermal lag. The melting temperature of the isothermally crystallized PLLA samples of different lamellar thickness was determined at atmospheric pressure and at elevated pressures using a DSC and a high pressure differential thermal analyzer (HP-DTA), respectively. The T_m at zero heating rate, (0 °C min^{-1}) was evaluated using the principle of "heating kinetics" to minimize thermal lag. Small angle X-ray scattering (SAXS) and the one dimensional correlation approach was used to determine the long period and the lamellar thickness of the crystals. The behavior of the T_m^o at elevated pressures will help to understand the crystallization behavior better.

2. Experimental

2.1. Materials

PLLA was supplied by Mitsui Chemicals, Inc., Japan. The sample was purified by dissolving it in chloroform and precipitating it from methanol and vacuum dried at 80 °C for several days before use. The M_w was 115,833, M_n 69,303 and M_w/M_n 1.67 determined from gel permeation chromatography (GPC) calibrated by polystyrene standards.

2.2. Sample preparation

Melt isothermal crystallization of PLLA was performed as follows: about 10 g of the polymer was melted at 220 °C for 5 min and pressed to a thickness of 1 mm using a hot press. The molten sample was quickly transferred to an annealing box equilibrated at a preset temperature. After 7 days (completion of crystallization), the sample was removed from the annealing box and quenched to room temperature. For high pressure measurements, about 8 mg of the polymer sample was melted directly in the aluminum DTA sample cup and crystallized following the procedure mentioned above for atmospheric pressure. Before high pressure analysis, the sample was coated with epoxy resin to prevent direct contact with the pressure transmitting silicon oil. Care was taken not to coat the Al cup in order to maintain high accuracy of the thermal signals and reduce noise. Fresh sample was used for each high pressure analysis because of the possibility of PLLA decomposing at high temperature required for melting at high pressures.

2.3. Measurements

2.3.1. Differential scanning calorimetry

Thermal analysis at atmospheric pressure was performed on a DSC (EXTER6200, SEIKO Instruments Inc., Japan) using about 7 mg of the isothermally crystallized samples. Heating was done from 20 to 220 °C at different heating rates, 5–20 °C min^{-1} with a nitrogen gas flow at 20 mL min^{-1}.

2.3.2. High pressure DTA

The high pressure DTA (Hikari High-Pressure Machinery Co., Ltd., Japan) apparatus was modified to suit our investigation. The heating rate was controlled by PID heater controller within ±0.1 °C. Type K (chromel-alumel) thermocouples were used to measure the temperatures of a sample and a reference material (aluminum). The sample cup, which was made from aluminum, was fitted directly onto the ceramic tube containing the thermocouple and the junction of the thermocouple was in direct contact with the aluminum cup just below the sample separated by 0.5 mm thickness of the aluminum cup as shown in Fig. 1.

At ambient temperature, desired pressure was applied and the temperature was raised at a heating rate of 10 °C min^{-1} while the pressure was maintained and monitored using a Heise gauge within ±1 MPa. The temperature of the sample and reference pans were recorded with a two channel recorder and the temperature difference between them was plotted against the reference temperature and the absolute minimum of the curve was taken as the melting temperature.

2.3.3. Small angle X-ray scattering (SAXS)

SAXS measurement was carried out using a Nano-Viewer (RIGAKU Corp., Japan). A Cu Kα radiation (40 kV, 20 mA) was used as an X-ray source. The two dimensional scattered intensity data were detected using an imaging plate (IP). The pinhole slits, samples, and IP were set in a vacuum chamber and the two

dimensional scattering pattern was measured under vacuum in order to eliminate air scattering. The lamellar thickness and the long period were estimated from the one-dimensional correlation function γ (r) given in equation (1):

$$\gamma(r) = \frac{\int_0^\infty q^2 I(q)\cos(qr)dq}{\int_0^\infty q^2 I(q)dq} \quad (1)$$

Here the denominator is the total integrated intensity or invariant Q and q is the reciprocal space scattering vector and is defined as

$$q = \frac{4\pi \sin(\theta)}{\lambda}$$

where 2θ is the scattering angle, and λ is the wavelength of the X-ray.

2.3.4. Specific volumes

Specific volume of PLLA as a function of temperature was measured using a confining fluid high pressure bellows type dilatometer (PVT Instrument, GNOMIX Inc., USA, which had a precision of ±0.0002 cm^3g^{-1}) from 10 to 200 MPa in the isothermal mode from 30 to 200 °C in steps of 10 °C and 10 MPa. The density of the sample at ambient condition was measured by an automatic gas pycnometer (Accupyc 1330, Micromeritics Instrument Corp., USA). The inverse of density was used as the initial value for the specific volume. The dilatometer sample cell, made from nickel sheet was filled with approximately 1 g of the polymer and mercury as a pressure medium. The cell was closed at one end by a flexible bellows and the change of specific volume was determined by the displacement of the bellows at various temperatures and pressures. The specific volume at atmospheric pressure was estimated by the Tait equation programmed in the instrument's software.

3. Results and discussion

3.1. Melting curves at atmospheric pressure

In general, the melting temperatures of polymers measured through thermal method depend on several factors: the heating rate, the crystal type, the mass and the lamellar thickness of the crystal. PLLA forms α′ crystals – a limited disordered modification when crystallized between 100 and 120 °C, compared to the normal α-form crystals when crystallized above 120 °C [27–29]. In addition, crystals formed at large supercoolings have smaller lamellar thickness which undergoes melting and reorganization during the heating scan [21]. Such melting and recrystallization processes disturb the measurement of the true melting temperature. To obtain α crystals only with thick lamellar crystals to minimize reorganization of the small crystals, PLLA was isothermally crystallized at higher temperatures. Fig. 2 shows the DSC heating curves of PLLA isothermally crystallized between 130 and 150 °C at a heating rate of 10 °C min^{-1}. The melting peak was observed to shift to higher temperatures with increasing T_c's indicating an increase in lamellar thickness. A shoulder melting peak appearing prior to the main melting peak is due to the melting of crystals with smaller lamellar thickness that may have formed during secondary crystallization. Multiple melting behavior has been reported for PLLA [30,31] when crystallized at different temperatures and heated at different rates. The small size of this peak suggests that a small portion of crystals with thin lamellae were present in the sample and has negligible effect on the main melting peak.

The heating rate in thermal analysis (DSC or DTA) also causes a shift of the T_m because of the high thermal resistance of polymers and thermal lag. Slower heating rates depress the shift while thin crystal lamellae tend to undergo reorganization (thickening) during the heating scan, which results in increase of the shift. The latter condition has been taken care of by using samples with thick lamellar crystals. Fig. 3 shows the heating rate dependence of T_m for samples isothermally crystallized at 140 °C. It can be seen that the peak melting temperature increased with heating rate.

Shift in T_m due to the thermal lag is corrected by taking the T_m at a heating rate of 0 °C min^{-1} and is termed as the corrected melting temperature (T_{mc}). T_{mc} is determined by extrapolating the T_m, determined at different heating rates to 0 °C min^{-1} [32,33]. The increase in the observed T_m caused by the thermal lag is proportional to the square root of the heating rate at constant thermal resistance, heat of fusion and sample weight on the basis of the theory of heat flow calorimetry. Ho et al. [33] proposed the equation for correcting the shift in T_m and is given in equation (2),

$$T = T_m - T_{mc} = (2W\Delta HRQ)^{1/2} \quad (2)$$

where Q is the heating rate, W is the sample weight used in DSC measurements, ΔH is the heat of fusion per gram of the sample and R is the thermal resistance of the sample. The other variables have been defined previously.

Fig. 4 shows the plot of T_m at atmospheric pressure scanned at

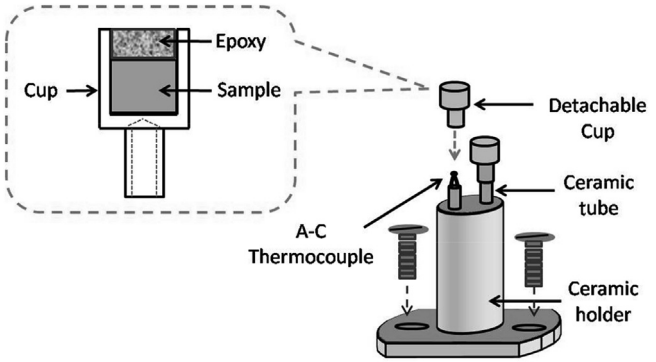

Fig. 1. Diagram of the high pressure DTA sample cup and ceramic holder.

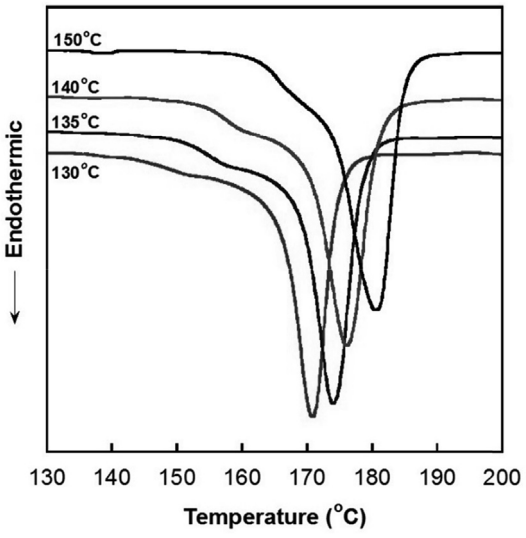

Fig. 2. DSC heating curves of PLLA isothermally crystallized between 130 and 150 °C at a heating rate of 10 °C min^{-1}.

different heating rates for the samples melt crystallized at various T_c as a function of the square root of the heating rate, $Q^{1/2}$. By linear extrapolation to 0 °C min^{-1}, the T_{mc} was obtained. The melting temperature difference between the heating rates at 0 and 10 °C min^{-1} for the samples crystallized at different T_c was found to be ca. 3.8 °C.

3.2. Melting curves at elevated pressures

HP-DTA melting curves of samples isothermally crystallized between 130 and 150 °C at atmospheric pressure were obtained at various pressures at a heating rate of 10 °C min^{-1}. Fig. 5 shows the DTA melting curve profiles of PLLA at various pressures for the samples isothermally crystallized at 140 °C. The T_m was found to shift to higher temperatures with increasing pressure. However, at a fixed pressure, the T_m was found to increase with increasing T_c, a behavior similar to that observed in DSC thermograms.

However, it was difficult to distinguish the shift in the T_m for different heating rates with the present HP-DTA, because the temperature resolution of HP-DTA used in this study was not very high as that of DSC due to noise and also due to the close proximity of the T_m at different heating rates. Therefore, the heating rate dependent T_m measurement at elevated pressures was not performed. The method to obtain T_m at zero heating rate at elevated pressures is explained later in the paper.

3.3. Equilibrium melting temperature

The T_m^o is commonly obtained by the following extrapolation methods: linear Hoffman and Weeks plot and the Gibbs-Thomson plot. Hoffman and Weeks method is based on the assessment of T_m of crystals grown at different T_c and is given as equation 3

$$T_m = \frac{T_c}{\beta} + T_m^o\left[1 - \frac{1}{\beta}\right] \quad (3)$$

where β is the crystal thickening factor which is assumed to be constant between the different samples crystallized at different T_c. The T_m of the sample is plotted against the T_c and the linear fit of the points is extrapolated to intersect the $T_m = T_c$ line. Both the T_m and T_c should be determined at the same pressure. Fig. 6 shows the

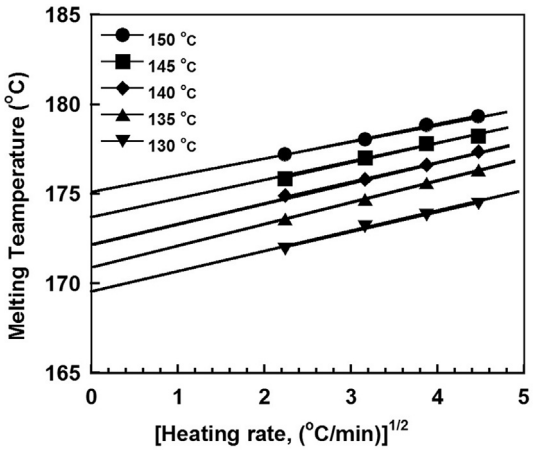

Fig. 4. The melting temperature of PLLA crystallized at different T_c against the square root of heating rate.

linear Hoffman-Weeks plot using T_{mc} against T_c at atmospheric pressure and the T_m^o was estimated to be 190 °C. This value is found to be within the range of reported values between 187 and 207 °C [3,34,35] using the same technique.

To estimate the T_m^o at elevated pressures using the linear Hoffman-Weeks method was impossible using the present HP-DTA apparatus because to crystallize PLLA at elevated pressures, high crystallization temperature was required for this polyester. Furthermore, due to the slow crystallization rate of PLLA, keeping this polymer at high temperature for extended time caused the polyester to degrade.

The alternative method was to use the Gibbs-Thomson plot and is given as equation (4). This method is reported for PLLA at atmospheric pressure [21].

$$T_m = T_m^o\left[1 - \frac{2\sigma_e}{l\Delta H_m^o}\right] \quad (4)$$

Here l is the lamellar thickness, ΔH_m^o is the enthalpy of fusion for the perfect crystalline phase, T_m is the observed melting temperature and σ_e is the surface energy of the crystalline lamellar [36].

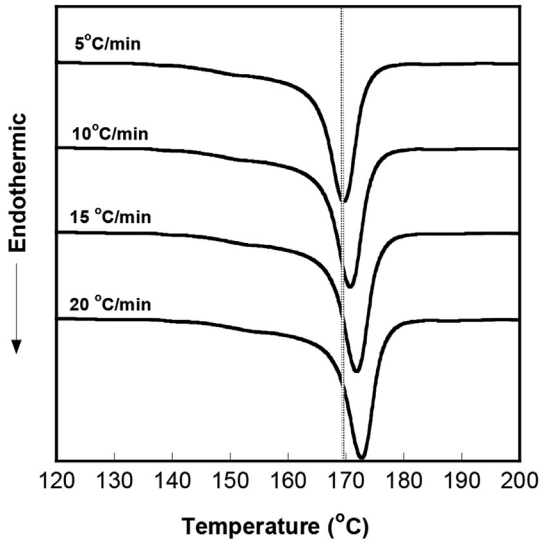

Fig. 3. DSC heating curves of PLLA at different heating rates for samples isothermally crystallized at 140 °C.

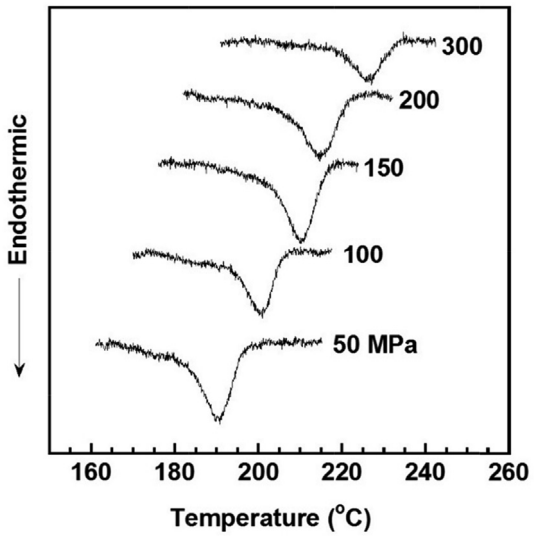

Fig. 5. HP-DTA heating curves at various pressures at a heating rate of 10 °C min^{-1} of PLLA isothermally crystallized at 140 °C at atmospheric pressure.

This equation predicts a linear relationship between T_m and $1/l$. T_m^o is determined by plotting the T_m vs the reciprocal of the lamellar thickness, $(1/l)$ and extrapolation of T_m to $l = \infty$ (intercept at $1/l = 0$).

From the SAXS profile of the PLLA samples crystallized between 130 and 150 °C, the electron density one-dimensional correlation function curve was derived and is represented in Fig. 7 for the sample crystallized at 140 °C. The curve exhibited a minimum followed by a maximum. The long period (Lp) was determined from the position of the first maximum of the correlation curve as shown in Fig. 7 and is the sum of the thicknesses of the crystalline lamellar (Lc) and the amorphous layer (La) i.e., (Lp = Lc + La). This is based on the assumption that the interface between the crystalline and amorphous phase is sharp. Lp was found to be 21.0 nm.

Using the "self correlation triangle method" [39] the thickness of one of the phase (L_2) was estimated by extrapolating the linear fit of the initial portion of the correlation function curve and intersected it with the horizontal line tangent to the first minimum peak as shown in Fig. 7. The point of intersection was found to be 6.4 nm. The thickness of the other phase (L_1) was then calculated to be 14.6 nm using the relation $L_1 = (Lp - L_2)$. Based on the crystallinity of the sample (57%), determined from density measurement, the larger fraction, L_1 was linked to the crystalline lamellar thickness and L_2 corresponded to the amorphous layer thickness. Lc was found to increase with increasing crystallization temperature and the relationship between Lc vs T_c fitted the second order regression polynomial according to equation (5).

$$Lc = 38.01 - 0.446T_c + 2.00 \times 10^{-3}T_c^2 \quad (5)$$

Here, the unit of Lc is in nm and T_c is in °C. The correlation coefficient was 99.6 and was the best fitting compared to the different orders. Similar curve fitting behavior has been observed in other polymers as well [37,38].

The T_m^o estimated by the Gibbs-Thomson method at atmospheric pressure using T_{mc} was 206 °C. This value is slightly higher than the reported value of 190 °C [21] using the same method. This difference could be due to the way the lamellar thickness was estimated from the one dimensional correlation function. It was noticed that a very small change in the lamellar thickness led to a significant difference in T_m^o.

For high pressure analysis, PLLA crystallized at atmospheric pressure was used because the lamellar thickness was known and was assumed to remain unchanged under elevated pressures when

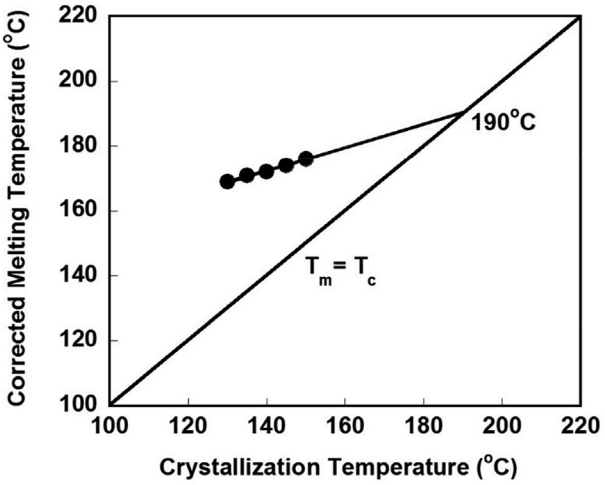

Fig. 6. Linear Hoffman Weeks plot using T_{mc}.

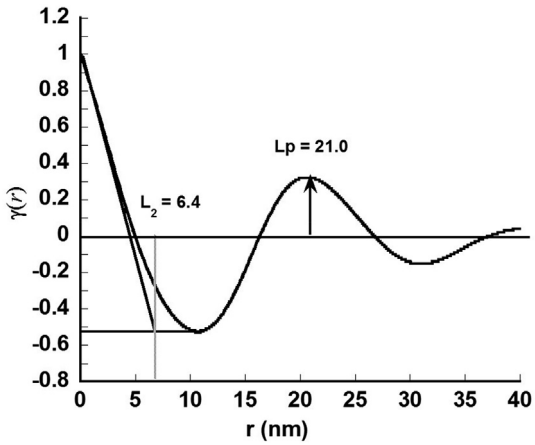

Fig. 7. Plot of the one-dimensional correlation function of PLLA crystallized at 140 °C from the melt.

the T_m was determined. This assumption will be verified later in the paper. It was difficult to determine the T_m at 0 °C min^{-1} at different pressures directly because of the close proximity of the T_m at different heating rates and the noise signals. Therefore, it was estimated by subtracting 3.8 °C from the T_m obtained at a heating rate of 10 °C min^{-1} at different pressures. This value of 3.8 °C was determined from the difference in the peak melting temperature obtained at 0 °C min^{-1} and 10 °C min^{-1} heating rate from DSC measurement at atmospheric pressure. Since the T_m of PLLA crystallized at different temperatures showed similar behavior at elevated pressures to that observed at atmospheric pressure, then at a fixed pressure, the melting temperature difference between 0 °C min^{-1} and 10 °C min^{-1} should be dependent on the heating rate and independent of pressure. Therefore, the correction was made.

Fig. 8 shows the plot of T_{mc} vs the inverse of lamellar thickness $(1/l)$ at atmospheric pressure and at elevated pressures. Since the T_m of the samples crystallized at various temperatures was at 0 °C min^{-1}, the slope of the T_m vs $1/l$ was independent of thermal lag.

The plot of T_m^o, estimated from Fig. 8 at various pressures against pressure is given in Fig. 9. The plotted points fitted the quadratic equation (6) of the following form:

$$T_m^o = 206 + 0.309P - 3.86 \times 10^{-4}P^2 \quad (6)$$

Here T_m^o is in °C and P is pressure in MPa. The regression coefficient was 99.8 indicating a good fit of the points. The T_m^o of 206 °C obtained from equation (6) at atmospheric pressure using the T_m at 0 °C min^{-1} for all pressures is analogous to that determined at atmospheric pressure using the Gibbs-Thomson equation. The pressure dependence of equilibrium melting temperature at atmospheric pressure, $\left(\frac{dT_m^o}{dP}\right)_o$ was found to be 0.309 K MPa^{-1}. This value is close to the $\left(\frac{dT_m^o}{dP}\right)_o$ values of PE [26] 0.30 K MPa^{-1} and PEG [40] 0.32 K MPa^{-1}.

However, if the T_{mc} estimated at atmospheric pressure and the T_m obtained at a heating rate of 10 °C min^{-1} at elevated pressures are used in combination to generate the plot, the quadratic equation (7), obtained has a very high pressure dependence coefficient.

$$T_m^o = 206 + 0.375P - 5.63 \times 10^{-4}P^2 \quad (7)$$

Therefore, it is suggested that the method of correcting the T_m at all

pressures to T_{mc} to determine the $\left(\frac{dT_m^o}{dP}\right)$ is more reliable.

One observation worth mentioning in Fig. 9 is the slope of the graph which increased almost linearly up to 200 MPa before curving inwards above 250 MPa. This feature has been observed for other polyesters as well [39]. Data up to 200 MPa fitted well to the linear equation and the $\left(\frac{dT_m^o}{dP}\right)_o$ was found to be 0.236 K MPa^{-1}.

To confirm if the 0.309 K MPa^{-1} obtained in this investigation was acceptable, it was compared with the value calculated from the Clapeyron equation (8) using reported values of the enthalpy of fusion.

$$\left(\frac{dT_m^o}{dP}\right)_0 = \left(\frac{\Delta V_f^o}{\Delta S^o}\right) = \left(\frac{T_m^o \Delta V_f^o}{\Delta H_f^o}\right)_0 \quad (8)$$

The specific volume change on fusion was obtained from dilatometry of the semicrystalline sample crystallized at 140 °C by measuring the difference between the specific volume in the melt and the semi-crystalline phase at T_m as shown in Fig. 10. T_m was defined as the midpoint where a large discontinuity in the specific volume occurred. The specific volumes in the melt and semi-crystalline phase at the T_m were estimated by extrapolation of the linearly dependent specific volumes with temperature. In the melt, specific volumes above T_m were used, while in the semi-crystalline state, the specific volumes between T_g and the pre-melting temperature (melting of premature crystals occurring far below the main melting peak) were used in the extrapolation. Plot of change in specific volume with increasing pressure followed a second order polynomial fit as shown in Fig. 11 with the following equation (9). Here P is in MPa.

$$\Delta V = 0.0347 - 1.99\text{x}10^{-4}P + 4.02\text{x}10^{-7}P^2 \quad (9)$$

Using this information, the volume change for perfect crystalline material was determined by adjusting it with the crystallinity determined from density measurement using equation (10).

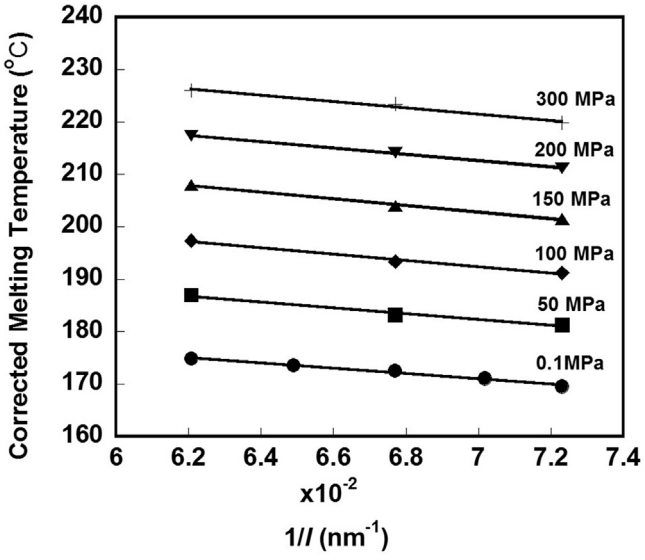

Fig. 8. Plot of T_{mc} at different pressures against the reciprocal of lamellar thickness (1/l).

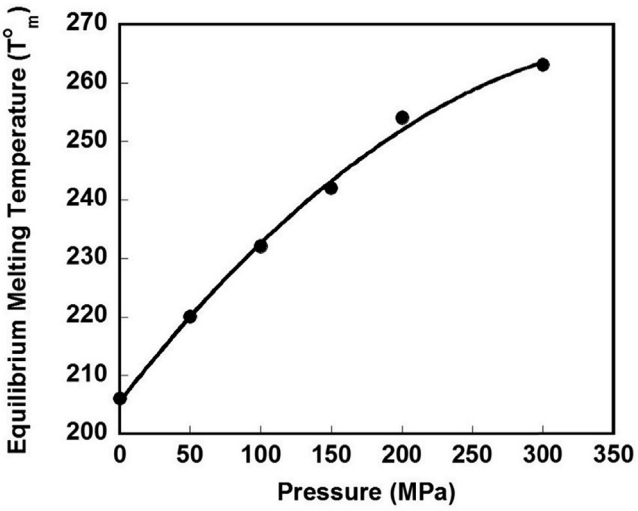

Fig. 9. Equilibrium melting temperature against pressure.

$$\chi_m = \frac{\rho_c(\rho - \rho_a)}{\rho(\rho_c - \rho_a)} \quad (10)$$

Here, χ_m is the mass crystallinity, ρ_a is the density of perfect amorphous, ρ_c, density of perfect crystalline and ρ, density of the sample. The crystalline and amorphous densities of the α crystal were 1.285 g cm^{-3} [41] and 1.245 g cm^{-3} [42], respectively and the density of the sample at atmospheric pressure at 26 °C was measured to be 1.267 g cm^{-3}. The change in specific volume of the sample with 57% crystallinity from the semi-crystalline state to the melt state (amorphous) was found to be 0.0347 cm^3 g^{-1}. For 100% crystallinity it was adjusted to 0.0609 cm^3/g. The enthalpy (ΔH_f^o) and entropy (ΔS^o) of fusion for the perfect crystal were also determined using the Clapeyron equation (equation (8)) by adjusting it with the degree of crystallinity and were found to be 94.5 Jg^{-1} and 0.197 Jg^{-1}K^{-1}, respectively. The ΔH_f^o has been reported

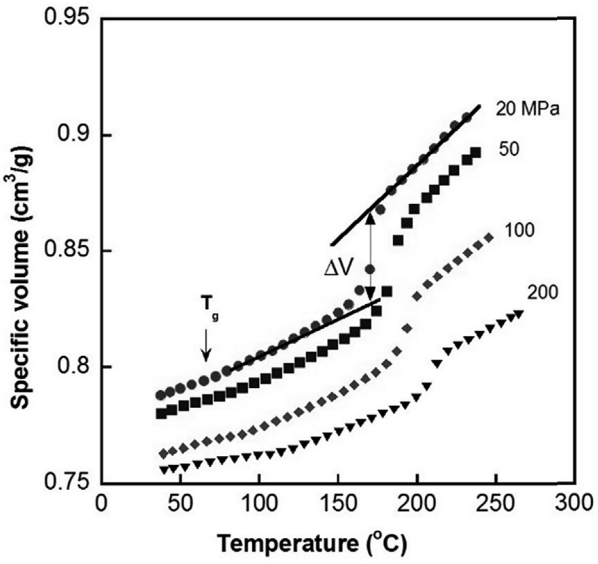

Fig. 10. Specific volume as a function of temperature at different pressures obtained in the isobaric mode. T_g and ΔV refer to the glass transition temperature and the change in volume at melting respectively.

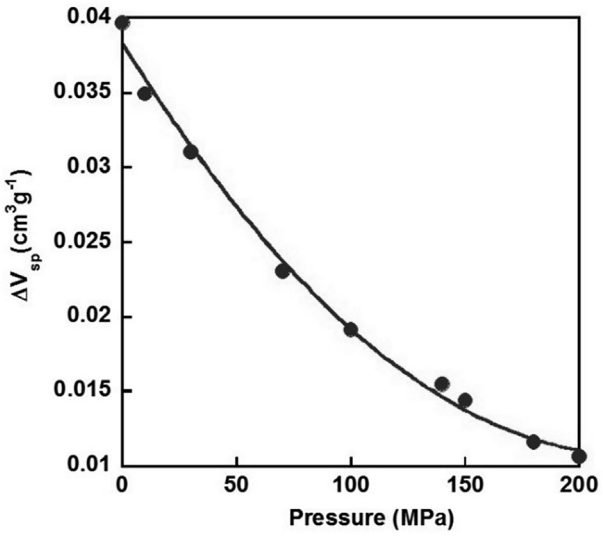

Fig. 11. Relationship of specific volume change of the sample crystallized at 140 °C with increasing pressure.

to be in the range of 93–140 Jg^{-1} using other techniques [4,41,42]. The result from this study is in good agreement with the lower range value. This also supports that the value of $\left(\frac{dT_m^o}{dP}\right)_o$ of 0.309 $KMPa^{-1}$ is also reliable.

Equation (4) provides one of the convenient ways of estimating the fold surface energy (σ_e). The σ_e of PLLA crystallized at atmospheric pressure was calculated to be 64×10^{-3} J m^{-2} and was obtained by multiplying the slope of T_m vs $1/l$ by the constant factor $\rho_c \Delta H_f^o / 2T_m^o$ where $\rho_c = 1.285$ g cm^{-3} [41] and $\Delta H_f^o = 94.5$ J g^{-1} and $T_m^o = 206$ °C (479 K) (obtained from this study). Our value is similar to the reported values in the range of $(100 \text{ to } 63) \times 10^{-3}$ J m^{-2} [43] which was obtained for different molecular weights and determined using the Lauritzen-Hoffman growth theory of crystallization in the regime II region [14]. In the regime II region, the secondary nucleation rate is considered to have the same order as the lateral growth rate (g) of the crystal and occurs at moderate supercoolings. σ_e was suggested to be molecular weight dependent. Since σ_e helps to enlighten what happens to the molecular chain at the fold surface (high σ_e value indicates loose-loop folds), it would be interesting to compare the σ_e of samples crystallized at elevated pressures. One way is to consider the slopes in Fig. 8 at elevated pressures. However, the issue with Fig. 8 is that atmospheric pressure crystallized samples were used for elevated pressure analysis. The similarity of the slopes at the different pressures up to 200 MPa suggests that the σ_e are analogous indicating that impact of pressure on the lamellar crystals was negligible. ΔH_f^o was calculated using the Clapeyron equation (8) at different pressures and are given in Table 1. It was found that up to 200 MPa, the ΔH_f^o and ΔS^o are quite similar but changes significantly at 300 MPa. This observation supports the method of using the lamellar thickness of atmospheric crystallized samples in constructing the Gibbs-Thomson plot at elevated pressures on the assumption that the lamellar thickness remained unchanged. The behavior of polymer properties changing around 300 MPa is consistent with other reports [21–25,44] and can be attributed to the thickening of the lamellar around 300 MPa as reported in PLLA [11] and some other polymers [21–26,45,46]. Since PLLA shows lamellar thickening behavior, it can be proposed that lamellar thickening of PLLA crystals may have occurred around 300 MPa before melting. This could be a reason for an increase in ΔV at 300 MPa and may contribute to a sudden increase in ΔH_f^o and ΔS. To verify this, the samples have to be crystallized at elevated pressures and measure the lamellar thickness. Unfortunately, due to the fast degrading nature of this polyester at high temperatures needed under high pressure, high pressure crystallization was not performed. Therefore, this proposal still remains to be answered.

Table 1
Pressure dependence of equilibrium melting temperature, change in volume, T_m^o, enthalpy and entropy of fusion at different pressures.

P (MPa)	(dT_m^o/dP)	ΔV (100%) x 10^{-2}	T_m^o(C)	ΔH_f^o(Jg^{-1})	ΔS° ($J\,K^{-1}g^{-1}$)
0.1	0.309	6.09	206.3	94.5	0.197
50	0.270	4.52	225.4	83.4	0.167
100	0.232	3.30	237.0	75.2	0.142
150	0.193	2.43	249.6	65.8	0.126
200	0.155	1.91	259.1	65.6	0.123
300	0.077	1.96	267.7	137.6	0.255

Nonetheless, the Gibbs-Thomson method used in this experiment to estimate T_m^o, $\left(\frac{dT_m^o}{dP}\right)_o$ and the thermodynamic variables of PLLA at various pressures are reliable.

4. Conclusions

The Gibbs-Thomson plot provided a good estimate of the equilibrium melting temperature of PLLA from atmospheric pressure and at elevated pressures. The pressure dependence of T_m^o followed the second order polynomial of the following form $T_m^o = 206 + 0.309P - 3.86 \times 10^{-4}P^2$ when T_m at zero heating rate at all pressures were used. The T_m^o and $\left(\frac{dT_m^o}{dP}\right)_o$ at atmospheric pressure were determined to be 206 °C and 0.309 K MPa^{-1}, respectively. The enthalpy and entropy of fusion of the perfect crystal at atmospheric pressure determined from the Clapeyron equation were 94.5 J g^{-1} and 0.197 J $K^{-1}g^{-1}$, respectively. These values were fairly similar up to 200 MPa suggesting that pressure had negligible effect on the lamellar crystals resulting in more or less similar slopes in the Gibbs-Thomson plot. The fold surface energy, σ_e, of the atmospheric pressure crystallized samples was calculated to be 64×10^{-3} Jm^{-2}. A significant increase in the enthalpy and entropy of fusion at 300 MPa suggests the pressure may affect the lamellar crystals which opens up more research.

References

[1] M.H. Hartmann, in: D.L. Kaplan (Ed.), Biopolymers from Renewable Resources, Springer-Verlag, Berlin, 1998, pp. 367–411.
[2] M. Yasuniwa, S. Tsubakihara, K. Iura, Y. Ono, Y. Dan, K. Takahashi, Polymer 47 (2006) 7554–7563.
[3] R. Vasanthakumari, A.J. Pennings, Polymer 24 (1983) 175.
[4] T. Miyata, T. Masuko, Polymer 39 (1998) 5515.
[5] D. Wu, L. Wu, Wu, X. Lanfeng, Z. Bin, Z.M. Yisheng, J. Polym. Sci. Part B Polym. Phys. 45 (2007) 1100–1113.
[6] J.F. Mano, Y. Wnag, J. Viana, Z. Denchev, M. Oliveira, Macromol. Mater. Eng. 289 (2004) 910–915.
[7] H. Tsuji, F. Horii, S.H. Hyon, Y. Ikada, Macromolecules 24 (1991) 2719–2724.
[8] J.M. Ahmed, K.V. Sunil, X.Z. Jian, S.R. Hosahalli, J. Food Eng. 9 (2009) 308–312.
[9] E. Bouthegourd, A. Esposito, A. Saiter, Macromol. Symp. 341 (2014) 26–33.
[10] T. Im, J.M. Gwon, S.H. Kim, Y.H. Shin, H.J. Kim, Chem. Eng. Data. 60 (2015) 2172–2177.
[11] J. Zhang, H.M. Yin, C. Chen, B.S. Hsiao, G.-P. Yuan, Z.-M. Li, J. Mater. Sci. 48 (2013) 7374–7383.
[12] M. Nofar, A. Tabatabaei, A. Ameli, C.B. Park, Polymer 54 (2013) 6471–6478.
[13] http://en.european-bioplastics.org).
[14] J.D. Hoffman, G.T. Davis, J.I. Lauritzen Jr., in: N.B. Hannay (Ed.), Treatise on Solid State Chemistry, vol. 3, Plenum, New York, 1976, p. 497.
[15] J.D. Hoffman, R.L. Miller, Polymer 38 (1997) 3151.
[16] K. Yamada, M. Hikosaka, A. Toda, S. Yamazaki, K. Tagashira, Macromolecules 36 (2003) 4802–4812.

[17] B. Wunderlich, Macromolecular Physics vol. 3, Academic press, New York, 1980.
[18] P. Juhász, J. Varga, K. Belina, H. Marand, J. Therm. Anal. Calorim. (2002) 561–574.
[19] P.C. Painter, M.M. Coleman, Essentials of Polymer Science and Engineering, Destech Publications Inc, 2008, pp. 309–311.
[20] Gert Strobl, The Physics of Polymers, Concepts for Understanding Their Structures and Behavior, third ed.s, Springer-Verlag, Berlin Heidelberg New York, 2007, pp. 191–204.
[21] T.Y. Cho, G. Strobl, Polymer 47 (2006) 1036–1043.
[22] S. Tsubakihara, A. Nakamura, M. Yasuniwa, Polym. J. 23 (1991) 1317–1324.
[23] H. Tanaka, T. Takemura, Polym. J. 12 (1980) 355–361.
[24] M. Yasuniwa, K. Haraguchi, C. Nakafuku, S. Hirakawa, Polym. J. 17 (1985) 1209–1219.
[25] C. Nakafuku, Polym. J. 27 (1995) 917–927.
[26] C. Nakafuku, Polym. J. 15 (1983) 641–647.
[27] J. Zang, Y. Duan, H. Sato, H. Tsuji, I. Noda, S. Yan, Y. Ozaki, Macromolecules 38 (2005) 8012–8021.
[28] M. Yasuniwa, K. Sakamo, Y. Ono, W. Kawahara, Polymer 49 (2008) 1943–1951.
[29] P. Pan, B. Zhu, W. Kai, T. Dong, Y. Inoue, Macromolecules 41 (2008) 4296–4304.
[30] M.L.D. Lorenzo, J. Appl. Polym. Sci. 100 (2006) 3145–3151.
[31] M.L.D. Lorenzo, Macromol. Symp. 234 (2006) 176–183.
[32] P.B. Rim, J.P. Runt, Macromolecules 17 (1984) 1520–1526.
[33] R.M. Ho, C.P. Lin, H.Y. Tsai, E.M. Woo, Macromolecules 33 (2000) 6517–6526.
[34] B. Kalb, A.J. Pennings, Polymer 21 (1980) 607–612.
[35] D.K. Gildings, A.M. Reed, Polymer 20 (1979) 1459–1464.
[36] E. Núñez, C. Ferrando, E. Malmström, H. Claesson, P.-E. Werner, U.W. Gedde, Polymer 4 (2004) 5251–5263.
[37] E.N. Dalal, K.D. Taylor, P.J. Phillips, Polymer 24 (1983) 1623–1630.
[38] D. Rohindra, K. Kuboyama, T. Ougizawa, Eur. Polym. J. 48 (2012) 1768–1776.
[39] G.R. Strobl, M. Schneider, J. Polym. Sci. Polym. Phys. 18 (1980) 1343–1359.
[40] C. Nakafuku, H. Yoshimura, Polymer 4 (2004) 3583–3585.
[41] S. Daisuke, T. Yasuhito, T. Masanori, K. Tetsuo, S. Moon, H.H. Suong, J. Polym. Sci. Part B Polym. Phy 45 (2007) 2632–2639.
[42] E.W. Fisher, H.J. Sterzel, G. Wegner, Kolloid-Z.u.Z. Polymere 251 (1973) 980.
[43] G.L. Loomis, J.R. Mudoch, K.H. Gardner, Polym. Prepr. Am. Chem.Soc., Div. Polym. Chem. 31 (1990) 55.
[44] D. Rohindra, K. Kuboyama, T. Ougizawa, Thermochim. Acta 545 (2012) 26–33.
[45] L. Li, R. Huang, A. Lu, W. Fan, S. Hong, Q. Fu, J. Cryst. Growth. 216 (2000) 538–541.
[46] J. Lu, R. Huang, Oh Il-Kwon, Macromol. Chem. Phys. 208 (2007) 405–414.